Seismic Performance of a 62-Story Steel Frame Hotel Tower

ERIC M. HINES and RICHARD A. HENIGE

Conceptual conflicts between code provisions and expected seismic behavior sometimes arise during the design process. This was the case during the 100% design development of a 62-story hotel/apartment tower, depicted in the center of Figure 1, for a site in Beijing, China. When it is constructed, the tower will reach a total height of 249.9 m (820 ft) above grade and terminate in a stone-clad, steel lantern structure. The highest occupied space will be at the 62nd story, 227 m (745 ft) above grade. Overall plan dimensions will be 40.0 m by 40.0 m (131 ft by 131 ft). The tower will carry lateral loads by means of a tube-in-tube structural system consisting of structural steel special moment frames on both the building and service core perimeters.

Circumstances prevented the coordination of consistent seismic design criteria between the design team and the owner, leaving the tower to be designed in accordance with building codes, Federal Emergency Management Agency (FEMA) recommendations for steel frames, and an external review panel in Beijing. The tower was designed to comply with the Chinese codes for the seismic design of buildings, *Code for Seismic Design of Buildings* (Ministry of Construction, 2001b), hereafter referred to as the Chinese Code, and *Technical Specification for Concrete Structures of Tall Buildings* (Ministry of Construction, 2001b). Additionally, the tower was designed to comply with the Chinese codes for wind forces (Ministry of Construction, 2001a), for tall steel structures (Ministry of Construction, 1998), and to satisfy the seismic design criteria of an expert review panel in Beijing. The tower was designed and checked with reference to the *International Building Code* (ICC, 2000), the AISC *Seismic Provisions for Structural Steel Buildings* (AISC, 2002), FEMA 350 (FEMA, 2000a), and FEMA 356 (FEMA, 2000b). Several conceptual conflicts arose during the design process between code provisions and expected seismic behavior. These conflicts are discussed to emphasize the importance of encouraging owners of tall structures to adopt rational seismic design criteria, independent of code requirements.

During the design process, peak ground accelerations for Beijing were assessed as 0.418g according to a site-specific seismic evaluation. These high seismic loads superseded wind loads in controlling the design of both the tower's stiffness and its strength. While the IBC 2000 requires such a tower to be designed as a special moment frame (SMF), pushover analyses suggested that inelastic rotation demands were on the order of the 2002 AISC *Seismic Provisions for Structural Buildings* requirements for intermediate moment frames (IMF). Furthermore, a capacity spectrum assessment under maximum considered earthquake (MCE) response spectrum loads showed that ductile capacity in the beams

Fig. 1. Hotel tower (center) and office towers (right and left), Beijing, China. (rendering courtesy of John Portman & Associates)

Eric Hines is a structural engineer, LeMessurier Consultants, Cambridge, MA, and research assistant professor, department of civil and environmental engineering, Tufts University, Medford, MA.

Richard Henige is vice president, LeMessurier Consultants, Cambridge, MA.

did very little to enhance the tower's performance because the Chinese Code acceleration response spectrum (ARS) was essentially flat for periods longer than six seconds. This fact implied that only added strength would improve the tower's ability to withstand MCE demands according to a capacity spectrum assessment, and thus contradicted the notion that adding ductility would significantly improve the seismic response of such a tower. Regardless of the accuracy of such an implication, its appearance in the Chinese Code significantly affected the design of the tower. This lack of clarity was further echoed in the assessment of column overturning forces according to pushover analyses. Although FEMA 350 (FEMA, 2000a, pp. 4–14) does not permit pushover analysis (nonlinear static procedure, NSP) for a tower of this height, the Beijing review panel permitted NSP for this tower to prove that displacement capacity far exceeded MCE displacement demands. Because linear time history analyses (linear dynamic procedure, LDP) demonstrated that the tower would not form hinges under five different MCE-level earthquakes, it was decided not to conduct a nonlinear time history analysis (nonlinear dynamic procedure, NDP) of the tower. In light of the computational effort required for an NDP under an earthquake amplified beyond the MCE level, the NSP was deemed adequate, and conservative for assessing the tower's overload performance. This pushover analysis conducted according to the tower's response in the fundamental mode produced overturning forces that were much higher than the overturning forces produced by MCE level time history analyses under artificial records. For such a tower, however, it is clear that higher mode effects can actually help the design by reducing overturning demands. As with the case of appropriate ductility capacity, however, it was not possible to use this information to make the tower design more economical while satisfying the relevant building codes.

LATERAL SYSTEM

The tower is designed to carry lateral loads by a tube-in-tube system with structural steel special moment frames on both the building and service core perimeters. All moment frame elements consist of built-up wide flange sections, with the exception of the corners of the perimeter frames, which are box sections. Typical service core moment frame columns are 900 mm (36 in.) deep by 400 mm (16 in.) wide. Web thicknesses vary from 60 mm (2.4 in.) at the base to 36 mm (1.4 in.) at the top of the building. Flange thicknesses vary from 100 mm (4 in.) at the base to 36 mm (1.4 in.) at the top of the building. The spacing of core columns varies from 1.70 m (5.6 ft) to 4.60 m (15 ft) to provide access to stairs, elevators, and ventilation ducts. Typical core girders are 900 mm (36 in.) deep by 300 mm (12 in.) wide. Web thicknesses vary from 19 mm (0.75 in.) at the base to 18 mm (0.71 in.) at the top of the building. Flange thicknesses are 20 mm (0.79 in.) throughout the building.

Typical perimeter columns are 1200 mm (48 in.) deep by 400 mm (16 in.) wide. Web thicknesses vary from 60 mm (2.4 in.) at the base to 30 mm (1.2 in.) at the top of the building. Flange thicknesses vary from 120 mm (4.7 in.) at the base to 40 mm (1.6 in.) at the top of the building. The typical spacing of perimeter columns is 5.00 m (16.4 ft). Corner columns are 800 mm (32 in.) square. Wall thicknesses for these hollow rectangular sections vary from 120 mm (4.7 in.) at the base to 25 mm (1 in.) at the top of the building. These dimensions were designed to conform to Chinese width/thickness ratios to prevent local buckling.

Until 75% design development (DD), two-story deep trusses from the 3rd story to the 5th story transferred loads from intermediate perimeter columns to eight 2.00 m (6.6 ft) square, confined, reinforced concrete columns. Below the 3rd story, wind and earthquake shear forces were transferred to 600-mm (24-in.)-thick, reinforced concrete, structural walls on the perimeter of the service core. Transfer trusses near the tower base were eliminated in the 100% design development at the request of the Beijing review panel to satisfy Chinese Code stiffness continuity criteria. This resulted in a fundamentally more flexible tower, especially at the base. Chinese stiffness continuity criteria are outlined in JGJ3-2002, *Technical Specification for Concrete Structures of Tall Buildings* (Ministry of Construction, 2002) as

$$K_i = \frac{V_i}{\Delta_{si}} \geq 0.7K_{(i+1)} \tag{1}$$

and

$$K_i = \frac{V_i}{\Delta_{si}} \geq 0.8\frac{K_{(i+1)} + K_{(i+2)} + K_{(i+3)}}{3} \tag{2}$$

where

K_i = story stiffness

V_i = story shear

Δ_{si} = story drift of the ith story

Ironically, these stiffness continuity criteria also became a primary motivator for the elimination of outrigger trusses at the 17th, 33rd, and 46th stories for the 100% DD package. Through 90% DD, outrigger trusses (see Figure 2) at these levels stiffened the tower approximately 17% by forming a shear connection between the service core and the perimeter frame. The stories located immediately under these stiff stories could not satisfy Equation 1. Therefore, although the spirit of Equation 1 [present also in Table 1616.5.2 of IBC 2000 (ICC, 2000)] is to prevent a soft story, it can be misused, as it was in this case by the design review board, to hinder the design of stiffer stories that are helpful to the lateral performance of high-rise structures.

Figure 2 compares the east perimeter frame and service core frame elevations for 75% DD and 100% DD, demonstrating the tendency under the direction of the Chinese review panel to shift the use of bracing from transferring loads and stiffening the overall system, to ensuring stiffness continuity. To satisfy the criteria given in Equations 1 and 2, lateral bracing was added to the lower stories near the base of the tower and on the story 33 mechanical level in the 100% DD package, as shown in Figure 2. These stories range in height from 4.5 to 5.5 m, and in the absence of outriggers and transfer trusses, their difference in stiffness from the typical 3.3-m-high stories exceeded the allowable levels.

ETABS MODEL

The hotel tower was modeled in three dimensions as a linear-elastic structural system using the analysis package ETABS (CSI, 1999). The 100% DD model consisted primarily of the perimeter and service core moment frames, the steel lantern structure, and the diagonal bracing. The global origin for the model was located at the foundation in the southwest corner of the perimeter frame, with the X-direction pointing to the east and the Y-direction pointing to the north.

Dead loads were applied from three sources. The self-weight of the frame was calculated by ETABS. The weight of the floor slabs, floor beams, partitions, mechanical equipment, and floor finish, were applied as uniformly distributed loads at each story level [4.95 kPa (103 psf)]. The weight of the curtain wall was applied as line loads to the beams in the perimeter frame [3.17 kN/m (217 lb/f)]. Live loads were applied as uniformly distributed loads at each story level [2.0 kPa (41.8 psf)]. The uniformly distributed dead and live loads were applied to shell elements connected to the perimeter and service core beams and columns. No floor beams or girders were included in the ETABS model, so the model's hierarchy of gravity load transfer differed slightly from that expected in the real structure for a given floor. Nevertheless, the distribution of axial loads in the columns was dominated by the vertical flexibility of the moment frames, rendering column demands in the ETABS model accurate on the whole.

Beam and column shear areas and moments of inertia were modified to reflect the true stiffness of these members as a result of their clear spans and joint shear deformations. Therefore, shear areas and moments of inertia increased for most members. Only the column shear areas had to be reduced in order to account for shear deformations in the beam-column joint.

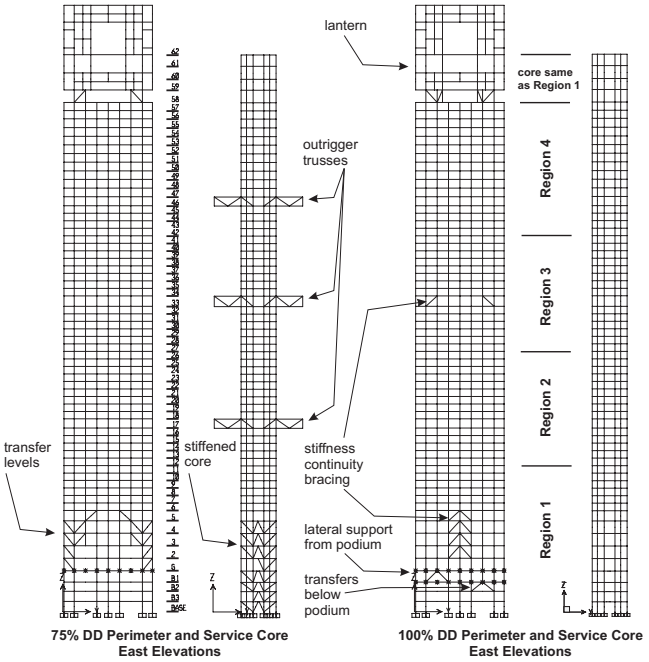

Fig. 2. Perimeter and service core frame east elevations.

LATERAL BRACING STRENGTH

Chinese Code requires checks on the building strength under 43 separate load combinations. In addition, 12 load combinations including vertical earthquake effects were evaluated by including the load case, $0.5E_V$. Results for these load combinations were compiled into maximum and minimum envelopes.

Diagonal braces were designed to resist the maximum forces resulting from the 12 earthquake load combinations plus the vertical earthquake load component, multiplied by the Chinese amplification factor 1.5, as shown in Equation 3.

$$1.5(1.2D + 0.6L + 1.3E_X + 0.28W_X + 0.5E_V) \quad (3)$$

Although most of the diagonal braces do not act explicitly as transfer members, all of the diagonal braces were designed conservatively to meet transfer member criteria.

NATURAL MODES AND MODAL MASS PARTICIPATION

To achieve approximately 90% modal mass participation in the vertical direction (UZ), the response spectrum analysis was conducted with 100 modes. Table 1 shows the first 12 modes, where translational modal mass participation in the horizontal directions (UX and UY) exceeds 90% by the 11th mode. This table shows, however, that vertical modal mass participation remains 0% in the first 12 modes, and indeed 90% vertical modal mass participation is reached only after the 89th mode.

Table 1. First 12 Modes and Modal Mass Participation Ratios for the 100% DD Design										
Mode (1)	Period (2)	UX (3)	UY (4)	UZ (5)	SumUX (6)	SumUY (7)	SumUZ (8)	RX (9)	RY (10)	RZ (11)
1	6.573	4.80	64.79	0.00	4.80	64.79	0.00	91.60	6.81	0.00
2	6.562	64.61	4.81	0.00	69.42	69.60	0.00	6.81	91.71	0.00
3	3.843	0.00	0.00	0.00	69.42	69.60	0.00	0.00	0.00	76.71
4	2.052	0.09	15.85	0.00	69.50	85.45	0.00	0.73	0.00	0.00
5	2.029	15.91	0.09	0.00	85.41	85.54	0.00	0.00	0.82	0.00
6	1.388	0.00	0.00	0.00	85.41	85.54	0.00	0.00	0.00	10.16
7	1.109	0.00	4.43	0.00	85.42	89.97	0.00	0.27	0.00	0.00
8	1.084	4.46	0.00	0.00	89.87	89.97	0.00	0.00	0.26	0.00
9	0.839	0.01	0.48	0.00	89.88	90.45	0.00	0.00	0.00	2.68
10	0.835	0.00	1.22	0.00	89.88	91.67	0.00	0.01	0.00	1.04
11	0.815	1.62	0.00	0.00	91.51	91.67	0.00	0.00	0.02	0.03
12	0.655	0.00	1.46	0.00	91.51	93.13	0.00	0.04	0.00	0.00

Table 2. Beijing Site PGA and Peak Spectral Accelerations as Fractions of Gravitational Force		
	Code	Site Specific
Design PGA	0.0720	0.0866
MCE PGA	0.405	0.418
Design Peak Sa	0.211	0.225
MCE Peak Sa	0.900	1.003

Table 3. IBC ARS Parameters for Site Class D											
IBC Site Class D, ARS Values											
F_a	F_v	S_s	S_1	S_{ms}	S_{m1}	S_{ds}	S_{d1}	$C_{smin(Des)}$	$C_{smin(MCE)}$	T_s	T_0
1.100	1.690	0.912	0.356	1.003	0.602	0.669	0.401	0.029	0.044	0.6	0.12

SEISMIC DEMANDS

Earthquake loads were evaluated according to Chinese and IBC standards. Table 2 gives peak ground accelerations (PGA) and peak spectral accelerations for the design earthquake and the maximum considered earthquake (MCE). Table 3 shows several IBC values for acceleration response spectra (ARS) with Site Class D. These values were created by matching S_{ms} to the Chinese site-specific ARS peak value and then calculating S_{m1} by multiplying S_{ms} by T_s = 0.6 s = site-specific report value for the MCE event on a site equivalent to the IBC Site Class D. Although the site-specific report applied T_s = 0.35 s for the design level earthquake, IBC values shown in this paper were all calculated according to T_s = 0.6 s. With S_{ds} = 0.669g > 0.50g, and S_{d1} = 0.401g > 0.2g for Site Class D, these earthquake demands place the tower in IBC's Seismic Design Category D.

Strength and stiffness of the tower under earthquake loads were evaluated according to the two Chinese ARS curves depicted in Figure 3. For reference, Figure 3 also shows the IBC design ARS for Site Class D and R = 3, which produces an IBC design spectrum that approximates the Chinese design spectrum, but which is clearly much larger than the spectrum required by IBC for a special moment frame. Figure 3 shows the Chinese Code design ARS to reach peak accelerations of 0.211g for periods of up to T_s = 0.35 s before descending first by an exponent of 0.95 and then linearly to 0.0296g for a period of T = 6 s. These values do not account for the Chinese earthquake load factor of 1.3. For periods greater than T > 6.0 s, the Chinese Code ARS remains flat at 0.0296g.

Table 4. Chinese and IBC ARS Values Compared for T = 6.6 s as Fractions of Gravitational Force					
Chinese Acceleration Values				IBC Acceleration Values	
Code		Site Specific		Site Class D	
Design	MCE	Design	MCE	Design	MCE
0.0296	0.157	0.00891	0.0717	0.0294	0.0912

In contrast to the Chinese Code ARS, the site-specific ARS gives 6.7% higher peak accelerations and, for longer periods, descends by an exponent of 1.1, where it finally gives accelerations that are 67% lower than the Chinese Code for T = 6 s. These low values result from the absence of a lower bound on the site specific ARS curve. Figure 3 includes the first three translational periods of the tower in both horizontal directions to reinforce the notion that the tower performs primarily in the longer period range where the code response spectrum dominates. While all analyses included torsion, torsional behavior is not discussed herein because it did not significantly influence the structural design. This is easily explained by the fact that the structure is both regular in plan and has a full perimeter moment frame as its primary lateral force resisting system. The IBC ARS curve shown in Figure 3 was created to match the peak accelerations of the Chinese site-specific ARS curve. This resulted in an almost perfect match between the IBC design ARS and the Chinese Code design ARS lower bounds (see also Table 4). The IBC ARS in Figure 3 reaches this lower bound at a period of T = 4.6 s. Therefore, accelerations for the hotel tower in its first two modes, which account for approximately 70% modal mass participation, are essentially the same according to the Chinese Code and the IBC, with the exception that the Chinese Code requires the forces resulting from these accelerations be multiplied by a load factor of 1.3.

Figure 4 shows IBC ARS curves for Site Class D, R = 3 and R = 8. This figure shows that, according to IBC, the design acceleration for the fundamental tower modes remains the same regardless of the site class and the seismic response modification factor. This similarity becomes more interesting when contrasted with the IBC requirement that steel intermediate moment frames (IMF) are limited in height to 49 m (160 ft) and IMFs are limited in height to 11 m (35 ft) in Seismic Design Category D. In category D, SMFs are allowed to be used above a height of 49 m (160 ft). In short, the IBC places a premium on ductile performance in exactly the type of structure for which it does not allow a reduction in design forces in response to this added ductility. Modes 7 and 8 fall within a region where there remains a clear distinction between demands on ductile frames and demands on frames with limited ductility, but Table 1 shows that these modes account for only 4.4% of the total mass participation. Figure 4 also shows that modes 4 and 5, which each account for approximately 16% modal mass participation, fall right on the border of the region where an increased R-factor allows for reduced acceleration demands. Although one may conclude from Figure 4 that higher modes are important for assessing

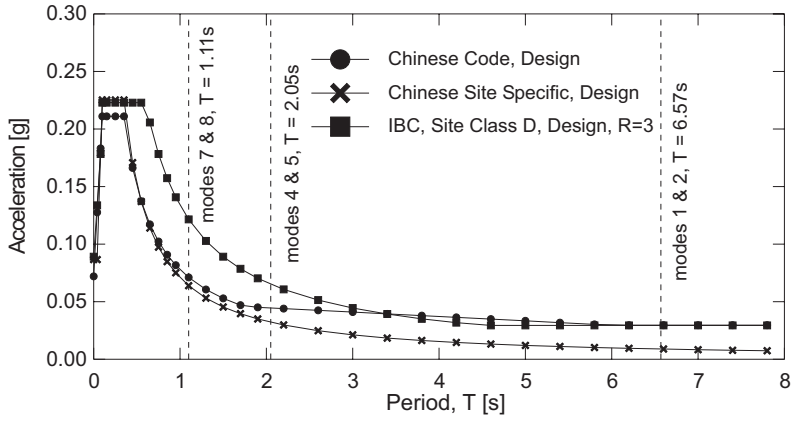

Fig. 3. Design acceleration response spectra, Chinese code GB 50011-2001 (Ministry of Construction, 2001b) vs. IBC 2000 (ICC, 2000).

the seismic response of the tower, they cannot completely characterize effects of ductility capacity on such a tower. At least two other essential considerations include: (1) the ability of ductile performance to modify favorably the tower's dynamic seismic response, and (2) the high overturning demands on the columns near the base of such a tower. Later sections will address both of these considerations.

Figure 5 shows the MCE ARS curves for the Chinese Code, the Chinese site-specific assessment, and the IBC. According to the authors' understanding of the Chinese Code, a structure is required to be designed for a lower level of acceleration and then checked according to plastic drift criteria under MCE acceleration. For the Chinese Zone 8, where the hotel tower is located, the peak spectral acceleration for short periods is specified as 0.16g for design and as 0.90g for the MCE event. Chinese Code requires the peak spectral acceleration to be modified by the damping correction factor given in Equation 4.

$$\eta_2 = 1 + \frac{0.05 - \zeta}{0.06 + 1.7\zeta} \tag{4}$$

where

ζ = percentage of critical damping

For the design level earthquake, where the Chinese Code stipulates that the tower shall remain elastic, $\zeta = 0.02$ yields a value of $\eta_2 = 1.32$. For the MCE earthquake, under which the tower is expected to form plastic hinges but relatively little global hysteretic damping (see Figure 9), $\zeta = 0.05$ yields a value of $\eta_2 = 1.00$. Dividing the Chinese MCE peak spectral acceleration by 1.32 to account for the damping correction factor, and 1.3 to account for the standard Chinese earthquake load factor, the relationship between the Chinese design ARS and MCE ARS curves becomes

$$\left(\frac{0.9g}{0.16g}\right)\left(\frac{1}{1.32}\right)\left(\frac{1}{1.3}\right) = 3.28 \tag{5}$$

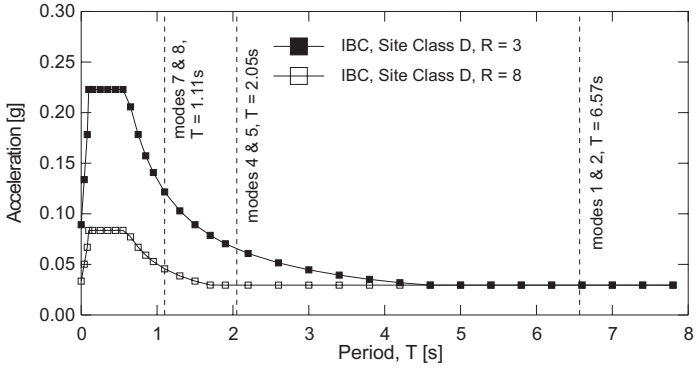

Fig. 4. Design acceleration response spectra, IBC Site Classes C, D, and E; R = *3, and* R = *8.*

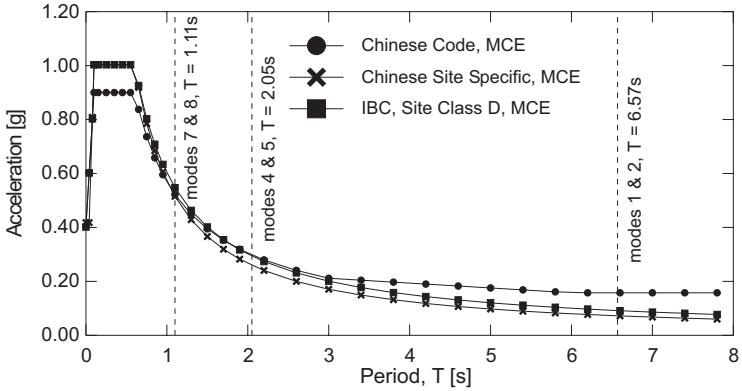

Fig. 5. MCE acceleration response spectra, Chinese Code, GB 50011-2001 (Ministry of Construction, 2001b) vs. IBC 2000 (ICC, 2000).

revealing that these two curves imply a seismic response modification factor of approximately $R = 3$.

AISC seismic requirements specify that columns be designed to carry overturning forces resulting from the factored load $\Omega_0 E$ in addition to dead and live loads according to the load combination

$$1.2D + 0.5L + \Omega_0 E + 0.2S_{DS}D \quad (6)$$

where

Ω_0 = 3.0

S_{DS} = design peak spectral acceleration for short periods

Consistent with the spirit of this requirement, columns were designed conservatively to carry forces that were determined from pushover analyses on the tower. Table 4 shows the wide spread of values that were possible to calculate for the design and MCE accelerations relevant to the first two translational modes of the tower. In this table and in Figure 5, none of the MCE accelerations include the ⅔ factor recommended by IBC for design accelerations, and none of the Chinese design accelerations include the load factor of 1.3. Therefore, the intention is that these values reflect actual MCE event values, not reduced or factored values applied for the purposes of design.

The interpretation of the values in Table 4 is further complicated by: (1) the extremely low values given for the Chinese site-specific ARS curves; (2) the inherent overstrength in such a tower is potentially higher than 3.0; and (3) the portions of the ARS curves in question are essentially flat. This third complication implies that no matter how ductile the structure is, changing its period by softening will not modify its dynamic response. These complications speak for the need for independent design criteria on such projects. Appropriate design criteria would allow desired performance to be achieved through a combination of strength and ductility that may not satisfy typical code standards but that can be demonstrated by analysis and testing to perform well. While such criteria are often applied to special structures, the Silver Tie Center provides a revealing glimpse of the issues that can occur on an international project where it was not possible to coordinate an independent set of criteria among the multiple interests involved. These interests included the American designers, the Chinese executive designers, the Chinese independent expert review panel, the Chinese Code, and the American synthesis, via the FEMA documents, of lessons for steel structures learned after the Northridge Earthquake. While obviously confusing, this situation is representative of several confusing situations created by the rapid development of earthquake provisions, and the general lack of detailed discussion regarding seismic performance of tall buildings.

LINEAR RESPONSE HISTORY ANALYSES

Figure 6 shows the story shears for the tower at 75% DD under forces calculated from the Chinese Code ARS and a suite of five time histories that include three artificial, site-specific records (B1, B2, and B3), along with El Centro and Taft records for comparison. The three site-specific records were synthetic records included with the geotechnical report for the project. These actual records produced spectral accelerations substantially lower than the Chinese Code design response spectrum. The review panel in Beijing, however, would not allow them to be used in lieu of the Code ARS, and subsequently required that they, along with El Centro and Taft records, be scaled such that the base shears resulting

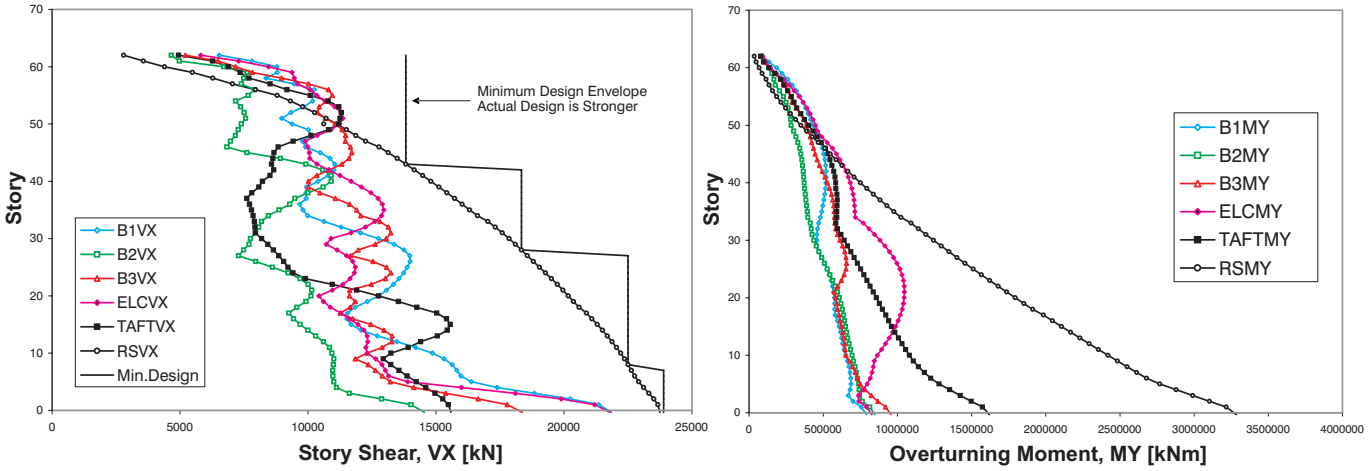

Fig. 6. Story shears and overturning moments under design loads in the global X-direction.

from individual records did not go below 65%, and the average base shear from all records did not go below 80% of the base shear calculated according to the Chinese Code ARS. The shears and overturning demands reported in Figure 6, therefore, do not reflect either the original design time histories or MCE time histories, but rather modified design time histories that satisfy the review panel's requirements.

Story shears under several modified response history load cases exceeded the story shears created by Chinese Code ARS at elevations higher than the 50th story, demonstrating the potential significance of higher mode effects. Member sizes at these heights were, however, consistent with member sizes at the 43rd story. At this level, the Chinese Code response spectrum predominated, exceeding the maximum story shear from El Centro above the 43rd story. Story shears from the artificial site-specific time history were roughly equivalent to the story shears produced by the site-specific response spectrum.

Figure 6 also shows the overturning moments under the same six load cases. This figure makes clear that the overturning moments, and hence the axial load demand in the columns due to horizontal loading, were significantly greater under the Chinese Code ARS than under any of the earthquake time histories.

In addition to assessing tower performance under modified design level time histories, the authors assessed tower performance under time histories with PGAs scaled by a factor of 4.82 from their design values to match the site-specific MCE PGA = 0.418g. If these linear MCE time history analyses had resulted in member demands that exceeded their elastic capacity, there may have been just cause to perform a nonlinear time history analysis of the tower. Member demands from the MCE linear time history analyses remained, however, below yield for all structural members. Table 5 lists the highest demands on perimeter frame beams under the MCE linear time history analyses.

Although higher mode effects could be observed in the story shears (see Figure 6), their impact was not serious enough to drive either the design or the analysis of the tower. Hence, the tower was designed elastically according to forces generated from the Chinese Code ARS. Columns were then designed to satisfy strong column-weak beam requirements and to carry overstrength axial load demands according to the pushover analysis and the Chinese Code ARS demands.

NONLINEAR STATIC PROCEDURE (PUSHOVER ANALYSIS)

Figure 7 depicts the basic properties of the plastic hinges applied to members in the perimeter service core frames. The numbers in Figure 7 relate specifically to beams with a 3800-mm (12.5-ft)-clear span in Regions 1 and 2 (see Figure 2) of the perimeter frame. The plastic rotation capacity of the hinge as $\theta_u = \theta_y + 6\theta_y$ applies, however, to all beam and column hinges in the ETABS model. The ETABS model calculated θ_y and M_p based on given member and section properties. Figure 7 also gives the magnitude of IMF plastic rotation capacity for the Region 1 perimeter frame beams. Figure 7 thus demonstrates that the allowable plastic rotation capacity in the model is closer to IMF capacity than to SMF capacity. Because demands did not approach SMF limits, discussion is provided here with respect to IMF limits to make the case that connections achieving IMF standards would be acceptable. Due to design criteria coordination difficulties mentioned earlier, however, it was not possible to incorporate this into the design criteria for the structure, and the connections were required to satisfy SMF criteria.

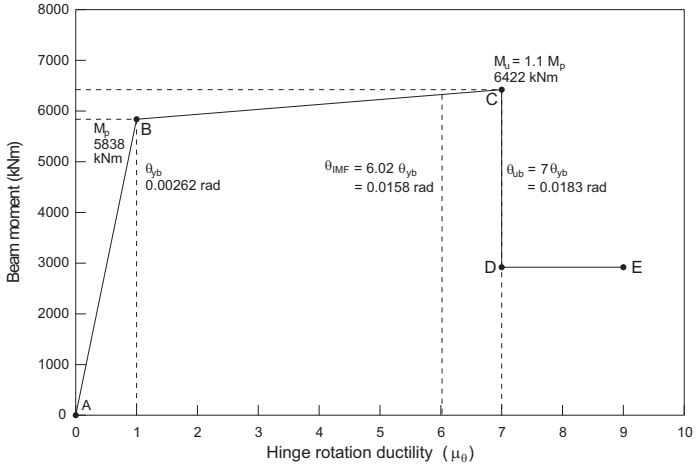

Fig. 7. Plastic hinge rotation capacity for perimeter frame beams in Region 1.

Table 5. Comparison of Perimeter Frame Beam MCE Maxium Moment Demands and Elastic Capacities							
	Taft [kNm]	**ElCentro [kNm]**	M_u **BTH1 [kNm]**	**BTH2 [kNm]**	**BTH3 [kNm]**	M_y **[kNm]**	M_{umax}/M_y
Region 1	3919	3511	2311	1457	1704	5106	0.77
Region 2	3214	2069	1568	1162	1405	5106	0.63
Region 3	2398	1962	1170	1012	1050	4542	0.53
Region 4	2281	2593	999	844	1072	3995	0.65

The magnitude of θ_{IMF} beam plastic hinge rotation capacity in Figure 7 was determined according to a beam-column subassembly plastic rotation of 0.01 radian, assuming that a beam hinge forms at the column face. Based on the kinematics of a plastic hinge concentrated entirely at the column face, the relationship between the beam column subassembly plastic rotation, θ_{pt}, and the beam plastic rotation θ_{pb}, can be calculated as

$$\theta_{pt} = \theta_{pb}\left(\frac{1}{1+\frac{d_c}{L_b - d_c}}\right) \tag{7}$$

Assuming that d_c = 1200 mm (47 in.) and $L_b - d_c$ = 5000 – 1200 = 3800 mm (150 in.), $\theta_{pt} = 0.76\theta_{pb}$. Note that the two assumptions—(1) the total plastic rotation for an IMF is equal to 0.01 radian, and (2) all of the plasticity is lumped at the column face—result in conservative estimates of the relationship between beam plastic rotation (as modeled in ETABS) and total subassembly rotation (as specified by AISC).

The moment-rotation curve in Figure 7 idealizes the moment-rotation behavior of the beam plastic hinge, by assuming that the member begins to yield once it reaches $M_p = ZF_{ye}$ at point B. Once the member has started to yield, its strength increases due to strain hardening to a maximum value of $M_u = 1.1M_p$ at a rotation demand of $\theta_{ub} = 7\theta_{yb}$. This implies that the beam is allowed to reach inelastic rotations of up to $\theta_{pb} = 6\theta_{yb}$. The short depth-to-span ratios in the hotel tower moment frames resulted in stiff beam-column subassemblies with relatively small yield displacements. Such small yield displacements allowed for significant rotational ductility within the limits of the IMF criterion $\theta_{pt} < 0.01$ radian. Note that all members were designed to yield in flexure prior to yielding in shear, assuming a point of inflection at midspan. Flexural yield rotation of a beam framed between two columns was defined as

$$\theta_{yb} = \frac{ZF_{ye}\, l_b}{6EI_b} \tag{8}$$

where

ZF_{ye} = M_p = plastic moment capacity of the member

l_b = $L_b - d_c$ = clear span between the columns

I_b = moment of inertia of the member about the axis of bending

This equation assumes that the flexural yield rotation is calculated as the flexural yield displacement divided by the member clear span as shown in Figure 8. For the perimeter frame beams in Region 1 with M_p = 5838 kN-m (51.7 kip-in.), l_b = 3.8 m (12 ft), E = 200,000 MPa (29,000 ksi), and I_b = 0.00707 m^4 (17,000 in.^{4}), the beam yield rotation is θ_{yb} = 0.00262 radian. Based on this value of θ_{yb}, Equation 7, and the assumption that 0.01 radian of total plastic rotation are allowed for the IMF, θ_{IMF} in Figure 7 may be calculated based on the value

$$\mu_{\theta b} = \frac{0.01\text{ rad}}{0.00262\,\text{rad}\left(0.76\right)} + 1 = 6.02$$

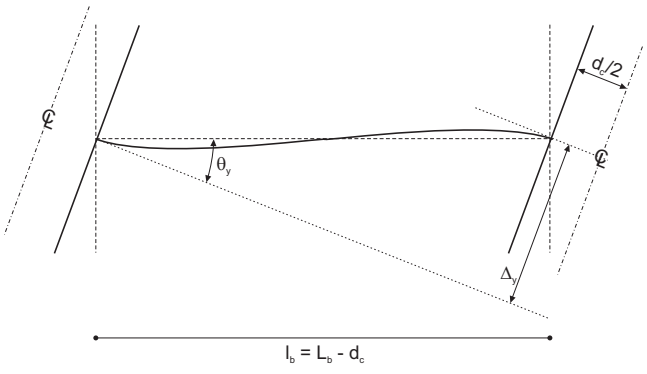

Fig. 8. Flexural yield rotation according to FEMA 356 (FEMA, 2000b).

Plastic hinges were further defined for several columns in the core and in the perimeter frames. These plastic hinges included both PMM hinges (hinges capable of accounting for the effect of axial load on moments about the *y*-axis and about the *z*-axis) and axial hinges. PMM hinge properties were defined according to Equations 9 and 10,

$$\theta_y = \frac{ZF_{ye}l_c}{6EI_c}\left(1-\frac{P}{P_{ye}}\right) \tag{9}$$

$$M_p = 1.18ZF_{ye}\left(1-\frac{P}{P_{ye}}\right) \le ZF_{ye} \tag{10}$$

where

$$P_{ye} = A_{gc}\,(325\text{ MPa})$$

Axial hinges were designed to yield when $P = P_{ye}$.

The tower was loaded in displacement control according to a lateral load pattern defined as the story shears from a response spectrum analysis of the tower calculated by combination of the first 18 modal responses according to the complete quadratic combination (CQC) method. Figure 9 show the nonlinear force-displacement response of the tower. Figure 10 shows plastic hinging in the tower under loads derived from Chinese ARS curves.

FEMA 350 (FEMA, 2000a) states on p. 3-77, "Where the clear-span-to-depth ratio of beams in the steel moment frame is less than 8, the qualifying total drift angle capacities indicated in Table 3-15 shall be increased to θ'_{SD} and θ'_{U}, given by Equations 3-70 and 3-71, respectively." For the moment frame in question, this provision would increase the qualifying strength degradation drift angle capacity for appropriate large-scale tests by a factor of 2.0 beyond the SMF requirements, in other words, 0.08 radian! It may not even be possible to achieve this level of ductility with such deep sections. Even if it were, this level of ductility is so far beyond the expected ductility demands on the actual structure, that there is no practical reason to adhere to this requirement in this specific case.

Figure 9 shows how little system ductility the tower actually has and how little it needs to satisfy demands derived from the Chinese Code MCE ARS, where the lower bound is very conservative. Additionally, the capacity spectrum analysis in Figure 11 shows that for the fundamental mode, increased ductility does not help the structure to meet the MCE demand criterion. In fact, if the same tower were to be designed to meet the Chinese Magnitude 9 MCE accelerations, no amount of additional ductility would help it meet the requirement. The response spectrum is so flat in this region, only added strength can drive the capacity of the structure above the required capacity. Figure 11 therefore raises two important questions: (1) Is it true that increased ductility is of no use to a long period structure performing in the fundamental mode? (2) Do minimum seismic lateral force demands on a long period structure in any way reflect the actual seismic demands expected on such a structure? The linear time history analyses discussed earlier seem to suggest that such minimum demands are unrealistic.

SUMMARY AND CONCLUSIONS

This paper has brought to light several conceptual conflicts encountered in both the Chinese Codes and the IBC during the design development of a 62-story hotel tower in Beijing,

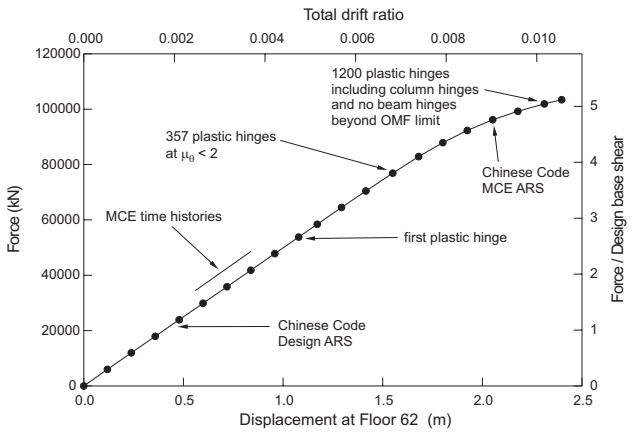

Fig. 9. Tower nonlinear force-displacement curve.

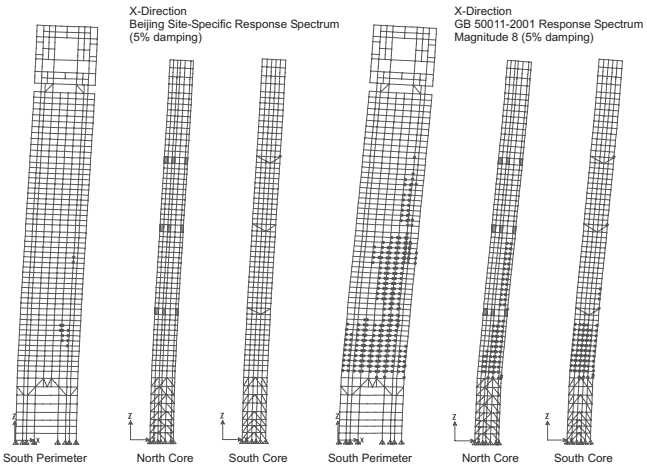

Fig. 10. Plastic hinging in the 75% DD tower perimeter frame and core under forces corresponding to the Chinese MCE site-specific and code ARS curves.

China. The conflicts revolve around the questions of: (1) the appropriate level of seismic demand on a tall building (defined as a building whose long period causes it to be subject to code minimum force requirements) and (2) the appropriate level of ductility for such a building. Earthquake acceleration response spectra generally decrease with increasing period, implying that for taller buildings earthquake loads are secondary to wind loads in driving such a building's design. Artificial lower limits on both Chinese Code and IBC ARS curves, however, ensured that design earthquake lateral forces predominated over wind lateral forces. Stiffness continuity criteria present in both the Chinese Code and the IBC led to a decision by the tower's seismic review panel in Beijing to forbid the use of outrigger trusses between the core and perimeter frames to stiffen the tower in the final design. While the authors did not conduct an exhaustive study of such stiffness concentration effects, it is worth noting that the review panel's decision to remove the outriggers was not based on any observations of poor dynamic behavior in tower configurations containing outriggers. In the end, the increased flexibility resulting from this decision allowed wind accelerations to develop in the upper floors that exceeded standard comfort criteria.

The IBC requirement that moment frame buildings taller than 49 m (160 ft) in Seismic Design Category D be detailed as SMFs, implied a large cost increase to the structure as a whole, while pushover analyses demonstrated that the ductility demand on the frame remained within the limits achieved by IMFs. The pushover analyses further implied that amplification of the column loads due to overturning under the MCE event would drive the column design near the base of the tower. These pushover analyses were based on a loading pattern consistent with the first mode only, and therefore neglected higher mode effects. Further nonlinear static studies that include more than one mode, such as the approaches discussed by Yu, Heintz, and Poland (2002), would likely offer deeper insight into the interaction of these higher modes with the fundamental mode in defining the limit state and overall force-displacement characterization of the tower. Linear time history analyses based on site-specific artificial ground motions showed that such higher mode effects would probably help the tower by reducing overturning demands. Furthermore, while these time history analyses did produce higher shears in the tower's upper stories, they did not produce ductility demand anywhere in the tower. The issues discussed in this paper suggest that the standard approaches of applying a minimum base shear and providing ductility capacity which are appropriate for shorter structures do not accurately reflect the seismic behavior of taller structures. Therefore, when dealing with tall structures, it is important for designers to encourage owners to adopt special design criteria that emphasize building performance over code requirements. Building codes and specifications could help in this matter by explicitly encouraging special design criteria for tall structures. Future research in support of such criteria should reconsider the age old minimum force requirement, with the question of whether or not it is appropriate for tall structures designed with robust, ductile systems.

ACKNOWLEDGMENTS

The authors would like to thank Albert Sun of John Portman Associates and Kent Yu of Degenkolb Engineers for their help in translating and interpreting the Chinese building codes.

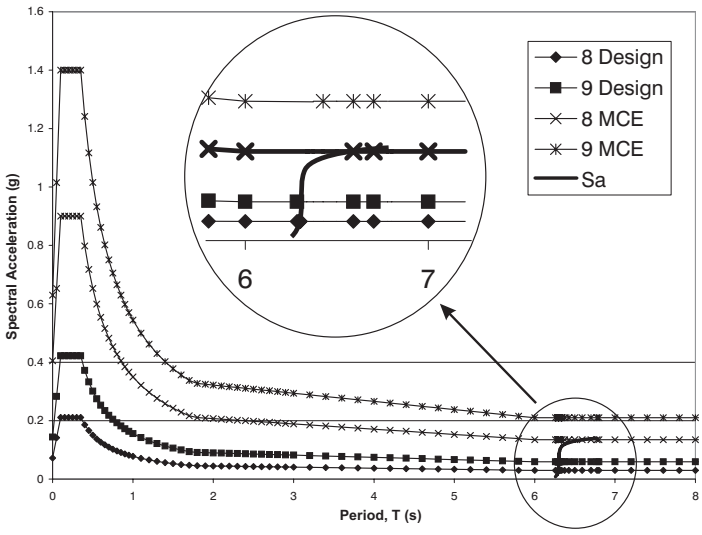

Fig. 11. Chinese Code capacity spectrum analysis of the nonlinear force-displacement curve.

REFERENCES

AISC (2002), *Seismic Provisions for Structural Steel Buildings*, ANSI/AISC 341-02, American Institute of Steel Construction, Inc., Chicago, IL.

CSI (1999), "ETABS: Three Dimensional Analysis and Design of Building Systems (User's Manual)," Computers and Structures, Inc., Berkeley, CA.

FEMA (2000a), *Recommended Seismic Design Criteria for New Steel Moment-Frame Buildings*, FEMA 350, Federal Emergency Management Agency, Washington, DC.

FEMA (2000b), *Prestandard and Commentary for the Seismic Rehabilitation of Buildings*, FEMA 356, Federal Emergency Management Agency, Washington, DC.

ICC (2000), *International Building Code*, International Code Council, Falls Church, VA.

Ministry of Construction (1998), *Technical Specification for Steel Structures of Tall Buildings*, JGJ 99-98, Architecture and Building Press, Beijing, China.

Ministry of Construction (2001a), *Load Code for the Design of Building Structures*, GB 50009-2001, Architecture and Building Press, Beijing, China.

Ministry of Construction (2001b), *Code for Seismic Design of Buildings*, GB 50011-2001, Architecture and Building Press, Beijing, China.

Ministry of Construction (2002), *Technical Specification for Concrete Structures of Tall Buildings*, JGJ 3-2002, Architecture and Building Press, Beijing, China.

Yu, Q.S., Heintz, J., and Poland, C. (2002), "Assessment of Nonlinear Static Analysis Procedures for Seismic Evaluations of Building Structures," *EERI 7th National Conference on Earthquake Engineering Proceedings*, Boston, MA, July.